

Supplementary Information

Supplementary Tables

- **ST1** Data demographics
- **ST2** Overall burden analysis results
- **ST3** Cortical gene set burden analysis results
- **ST4** Summary statistics on gene count and number of CNV carriers
- **ST5** Summary statistics on cortical gene set effect sizes
- **ST6** Correlation between deletion and duplication effect size profiles
- **ST7** Correlation between the 20 neuromaps and deletion and duplication effect size profiles
- **ST8** Summary statistics on effect sizes for sensorimotor and association cortical axes
- **ST9** Del/Dup profile stability. Correlation between effect size profiles (del-del and dup-dup) across all pairs of analysis.
- **ST10** Fold change between regional specificity thresholds of $Z > 0.2$ and $Z > 1.0$ for sensorimotor and association cortical axes
- **ST11** GO-term enrichments in Glasser 180 cortical gene sets
- **ST12** Correlations between GO term enrichment profiles (across Glasser 180 cortical gene sets) and deletion/duplication effect size profiles

Supplementary Figures

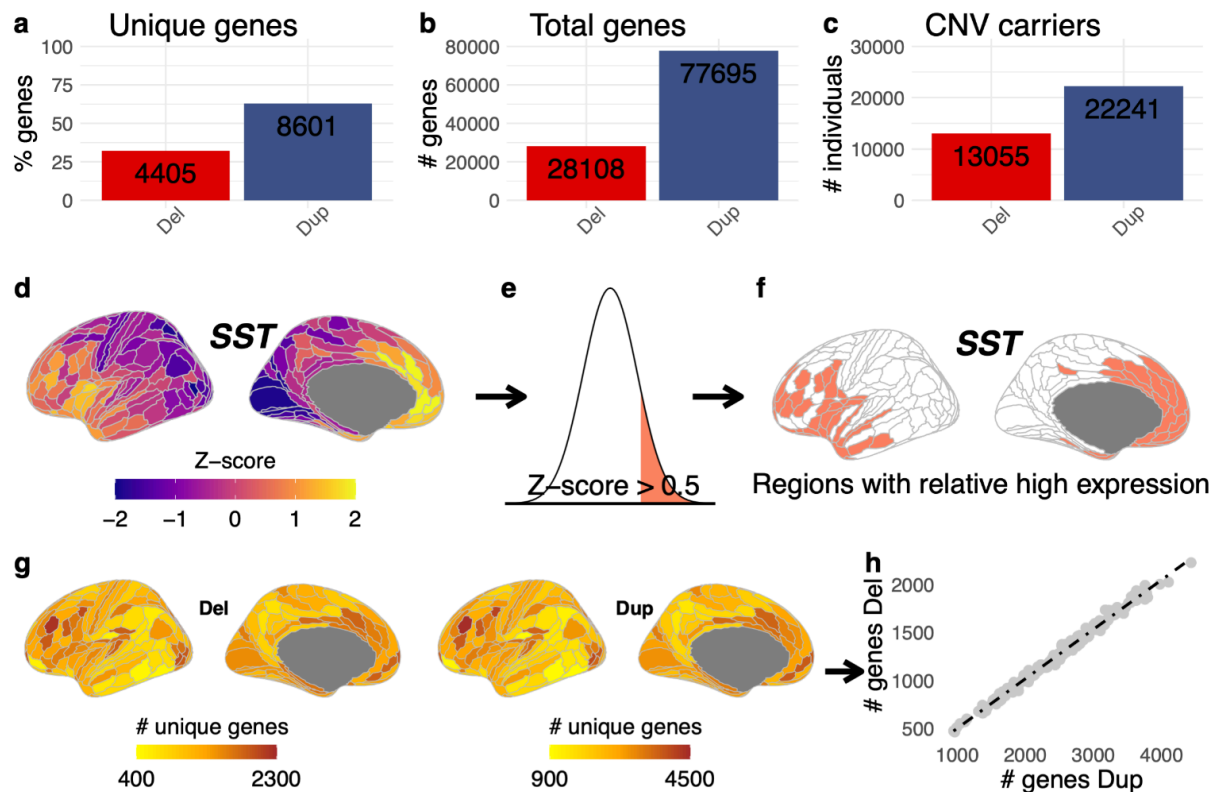


Fig. S1. Summary of CNV carriers.

Legend: **a-c**), Barplot showing the percentage of unique genes, number (#) of total genes (accounting for recurrence), and CNV carriers observed in deletions and duplications in our assembled data, covering 32.2% and 62.9% of 13678 genes with spatial expression data (AHBA) and have been detected in the brain (HPA). **d-f**), Method to identify genes with relative high expression across cortical regions. Method to establish relative high expression. As an example, the expression of **d**), SST is z-scored across 180 cortical regions. We then **e**), thresholded the Z-score to **f**), identify the cortical regions with relative high expression of SST. This procedure was applied across all 13,678 genes, resulting in 180 lists of relatively highly expressed genes (RHEXG) corresponding to each cortical region of the Glasser parcellation. **g**), The number of unique RHEXGs per cortical region for deletions and duplications. Separate color bars highlight the difference in the range of values between

deletions and duplications for both unique and total genes per cortical region. **h)**, Scatterplot showing a high degree of similarity in the distribution of the number of unique genes per cortical region between deletions and duplications. Each point represents a cortical region, with unique genes per cortical region for deletions and duplications on the Y-axis and X-axis, respectively.

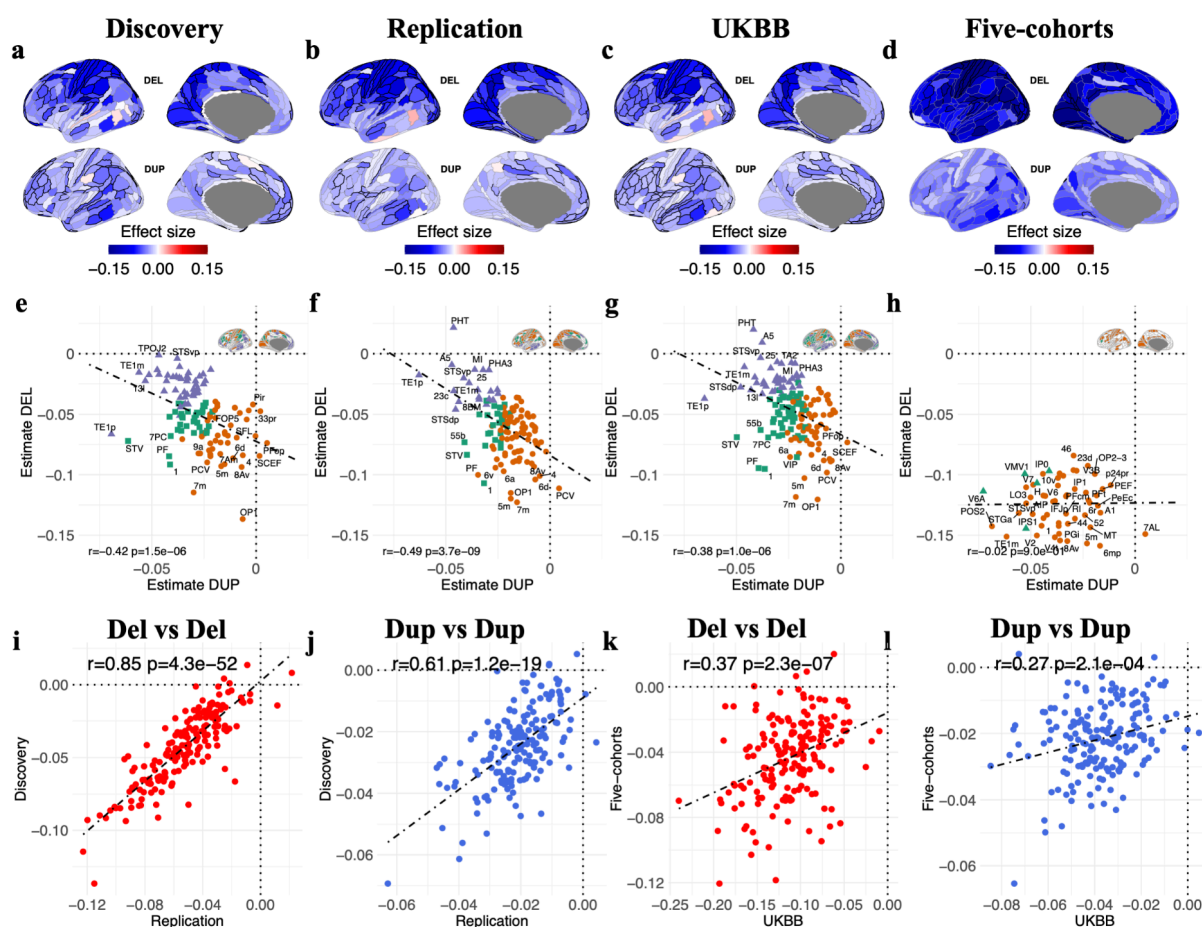


Fig. S2. Replication in data subsets.

Legend: Brain maps showing the spatial distribution of effect sizes per cortical region for deletions and duplications for **a)** discovery; **b)** replication; **c)** UK Biobank; and **d)** five general population cohorts excluding UKBB.

Scatterplots showing correlation between the effect sizes of deletions and duplications across the cortex for **e)** discovery; **f)** replication; **g)** UK Biobank; and **h)** five cohorts. Each point is the mean effect size of genes in each of the cortical regions. X-axis: duplication; Y-axis: deletion effect sizes, respectively. Only significant effects are plotted, and corresponding significant regions are shown as a brain-plot in the top right corner.

Scatterplots showing correlation between the effect sizes across the cortex for **i)** deletion-discovery vs deletion-replication; **j)** duplication-discovery vs duplication-replication;

k) deletion-UKBB vs deletion-Five-cohorts; and **l)** duplication-UKBB vs duplication-Five-cohorts. Each point is the mean effect size of genes in each of the cortical regions.

Del: deletion; Dup: duplication; #: number.



Fig. S3. Replication in independent gene expression RNA-seq resources

Scatterplot showing correlation between the effect sizes of deletions and duplications across the cortex for **a)**, analyses using gene expression data from the Human Protein Atlas¹ (73

cortical regions); $r=-0.53$, FDR corrected parametric p-value= $1.8e-4$. **b)** analyses using gene expression data from the BrainSpan² adult (11 cortical regions); $r=-0.85$, FDR corrected parametric p-value= $7e-3$.

Del: deletion; Dup: duplication; r: Pearson correlation.

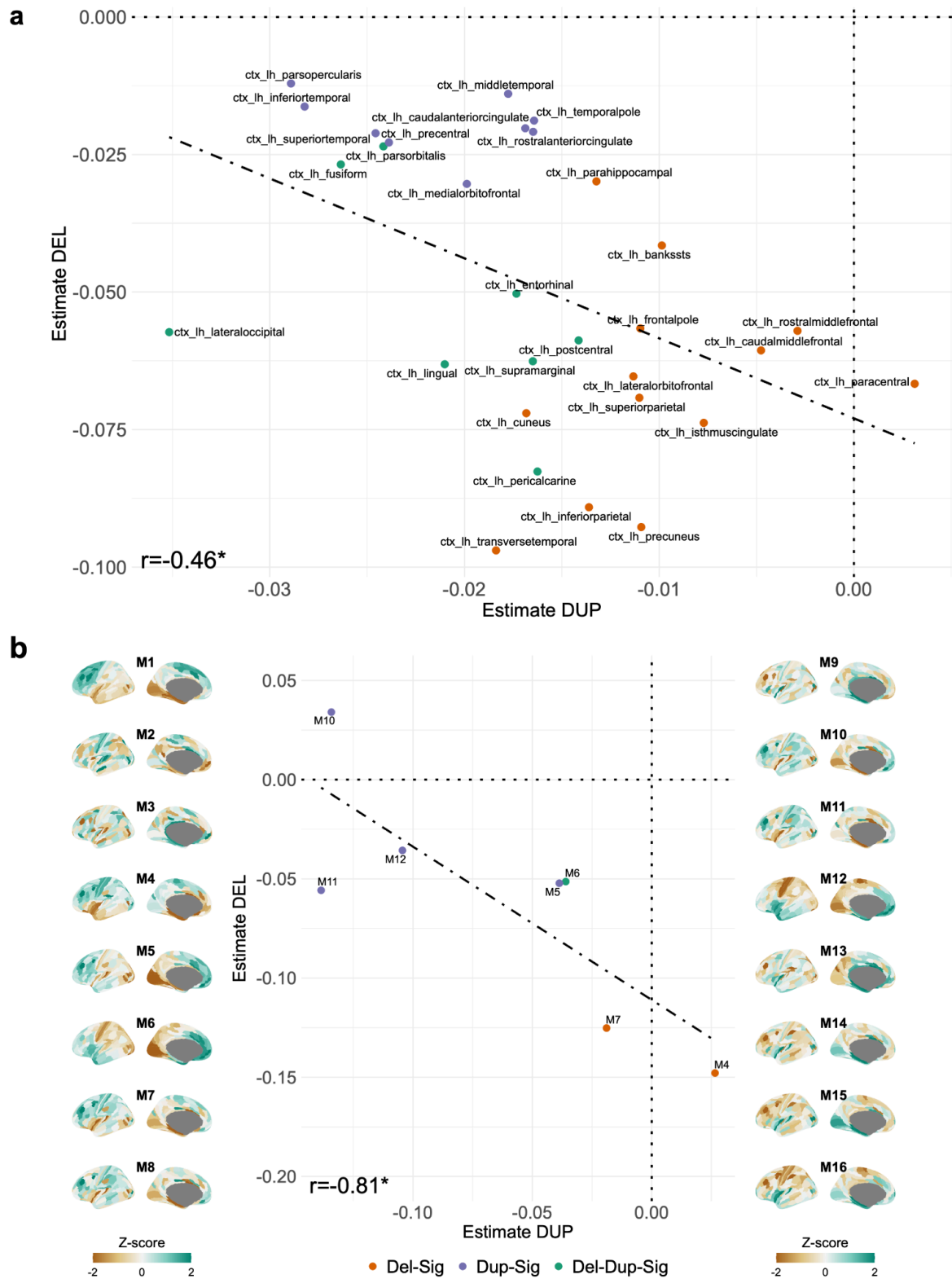


Fig. S4. Replication in alternative methods for defining cortical gene sets from AHBA

Scatterplot showing correlation between the effect sizes of deletions and duplications across the cortex for a) independent processing of Allen Human Brain Atlas from French and Paus³,

by averaging expression for probes within Desikan parcellation (34 cortical regions, alternative processing of AHBA gene expression data than the abagen package⁴ used in main analysis). Correlation between deletion and duplication effect sizes: $r=-0.46$, FDR corrected spin permutation p-value= $2.2e-2$. Gene-sets were defined by Z-scoring the expression and then applying a threshold. **b)** independent analyses of Allen Human Brain atlas, defining 16 spatial modules of cortical gene expression from Wagstyl et al.⁵ We used the module genes as gene sets (16 modules, expression profile of PC1 of the 16 modules shown on the sides of panel b). Correlation between deletion and duplication effect sizes: $r=-0.46$, FDR corrected spin permutation p-value= $2.7e-2$.

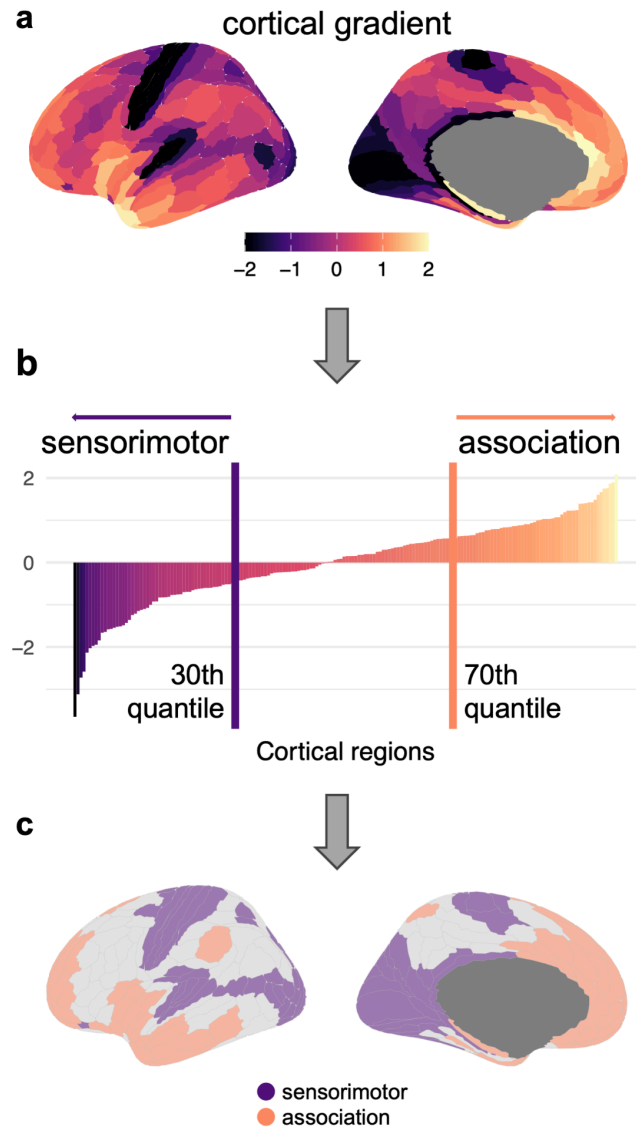


Fig. S5. Assigning cortical regions to sensorimotor and association axes

Assigning cortical regions to the sensorimotor (unimodal) and association (transmodal) axes using the approach from Seguin et al^{6,7}. **a)** Cortical regions were ranked based on previously established sensorimotor-association axis: anatomical hierarchy⁸ (T1w/T2w ratio). **b)** We examined the effect sizes of the top and bottom 30% of these regions (Seguin et al^{6,7}). **c)** The sensorimotor and association cortical regions are colored in dark purple and light orange, respectively.

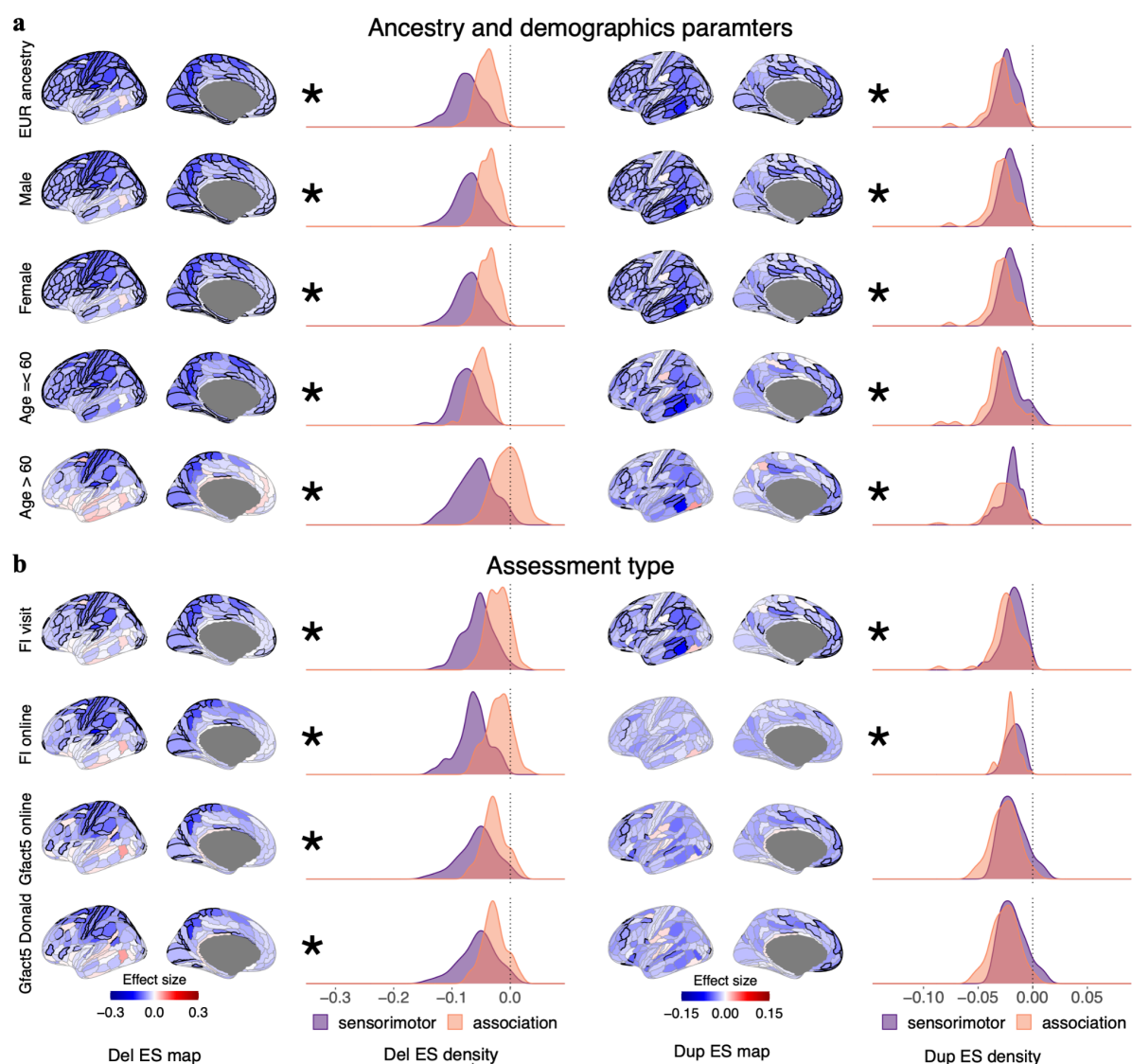


Fig. S6. Characterizing the impact of age, sex, ancestry, and assessment type.

Legend: Effect sizes maps of cognitive ability and density plots comparing effect sizes of sensorimotor and association regions for deletions (left) and duplications (right) for **a)** analyses ran with participants of European ancestry, male, female, age ≤ 60 , and age > 60 ; **b)** analyses ran with subset of participants based on assessment type: FI visit (UK Biobank Fluid intelligence score from Assessment centre visit, Data-Field 20016), FI online (UK Biobank Fluid intelligence score from online assessment, Data-Field 20016), Gfact5 online

(g-factor for 5 cohorts and UK Biobank online); Gfact5 Donald (g-factor computed using another approach). Del: deletion; Dup: duplication; ES: effect size; FI: fluid intelligence; Gfact: G-factor. * : represents significant difference between the sensorimotor and association effect sizes; Kolmogorov–Smirnov test p-value < 0.05 (FDR corrected).

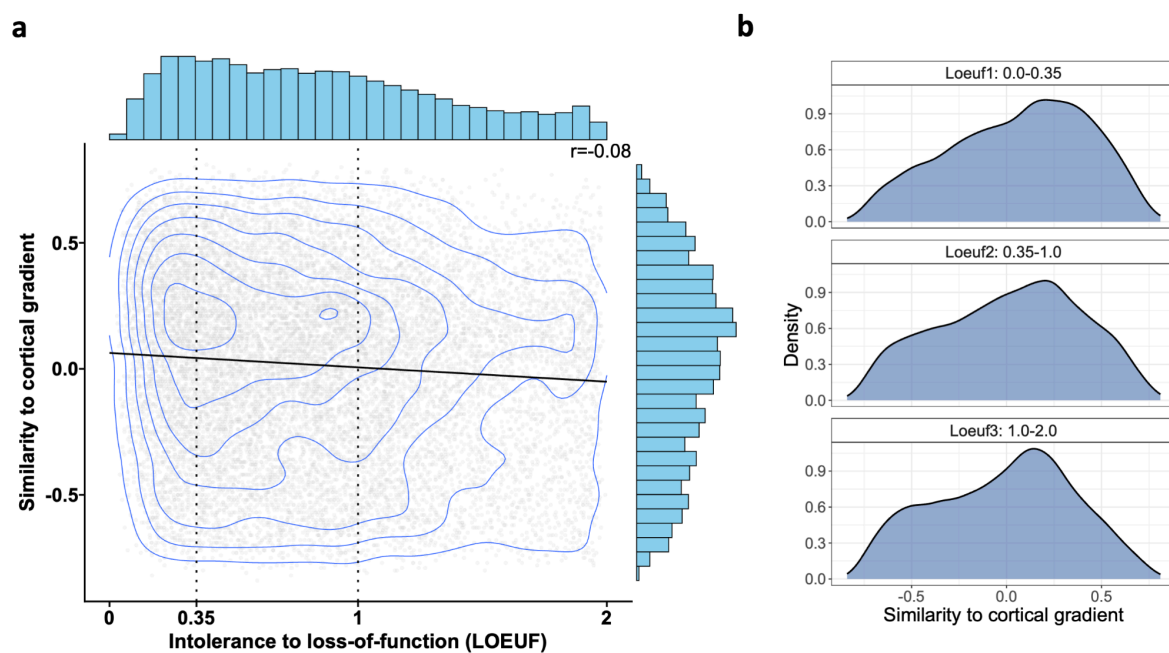


Fig. S7. Correlation between genetic constraint and similarity to cortical gradient.

a) Correlation between values of genetic constraint (X-axis: intolerance to Loss of Function, LOEUF) and a measure of spatial expression (similarity of gene expression to cortical gradient). Each dot represents a gene expressed in the cortex. The contours are 2-dimensional density plots. **b)** Density plots for similarity to cortical gradient values for genes stratified into three LOEUF categories: i) highly intolerant (Loeuf1: 0-0.35); ii) intolerant (Loeuf2: 0.35-1.0); and iii) tolerant (Loeuf3: 1.0-2.0).

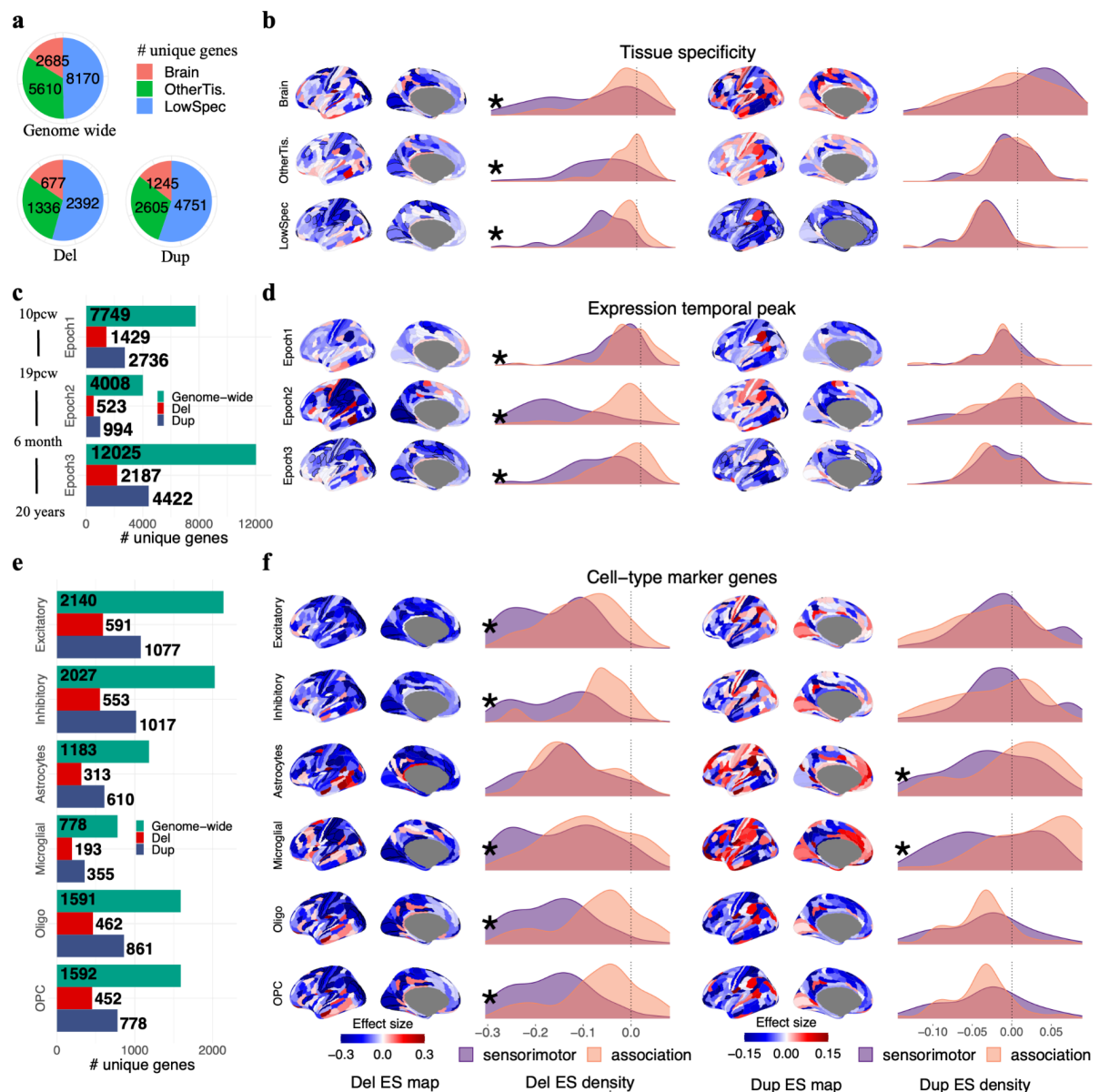


Fig. S8. Characterizing the impact of tissue-specificity, temporal dynamics of gene expression, and cell types.

a) Pie charts showing the distribution of genes with elevated expression in the brain (red), elevated expression in non-brain tissues (green), and low tissue specificity (blue). Number (#) of unique genes observed in deletions and duplications in our assembled data, as well as genome-wide (reported in the Human Protein Atlas). **b)** Effect sizes maps of cognitive ability and density plots comparing effect sizes of sensorimotor and association regions for

deletions (left) and duplications (right) for the three non-overlapping categories of tissue specificity.

c) Barplot showing the number of genes with peak expression during epoch1 (10pcw to 19pcw), epoch2 (19pcw to 6 months after birth), and epoch3 (6 months onwards). Number (#) of unique genes observed in deletions (red) and duplications (blue) in our assembled data, as well as genome-wide (green, as reported in the BrainVar resource). **d)** Effect sizes maps of cognitive ability and density plots comparing effect sizes of sensorimotor and association regions for deletions (left) and duplications (right) for the three non-overlapping categories of expression temporal peaks.

e) Barplot showing the number (#) of cell-type marker genes, across 6 categories, observed in deletions (red) and duplications (blue) in our assembled data, as well as genome-wide (green, reported in the Human Protein Atlas, HPA). **f)** Effect sizes maps of cognitive ability and density plots comparing effect sizes of sensorimotor and association regions for deletions (left) and duplications (right) for the six overlapping cell-type marker categories.

* : represents significant difference between the sensorimotor and association effect sizes; Kolmogorov–Smirnov test $p\text{-value} < 0.05$ (FDR corrected). Del: deletions; Dup: duplications; ES: effect size; HPA: Human Protein Atlas; r: Pearson correlation; Sig: significant.

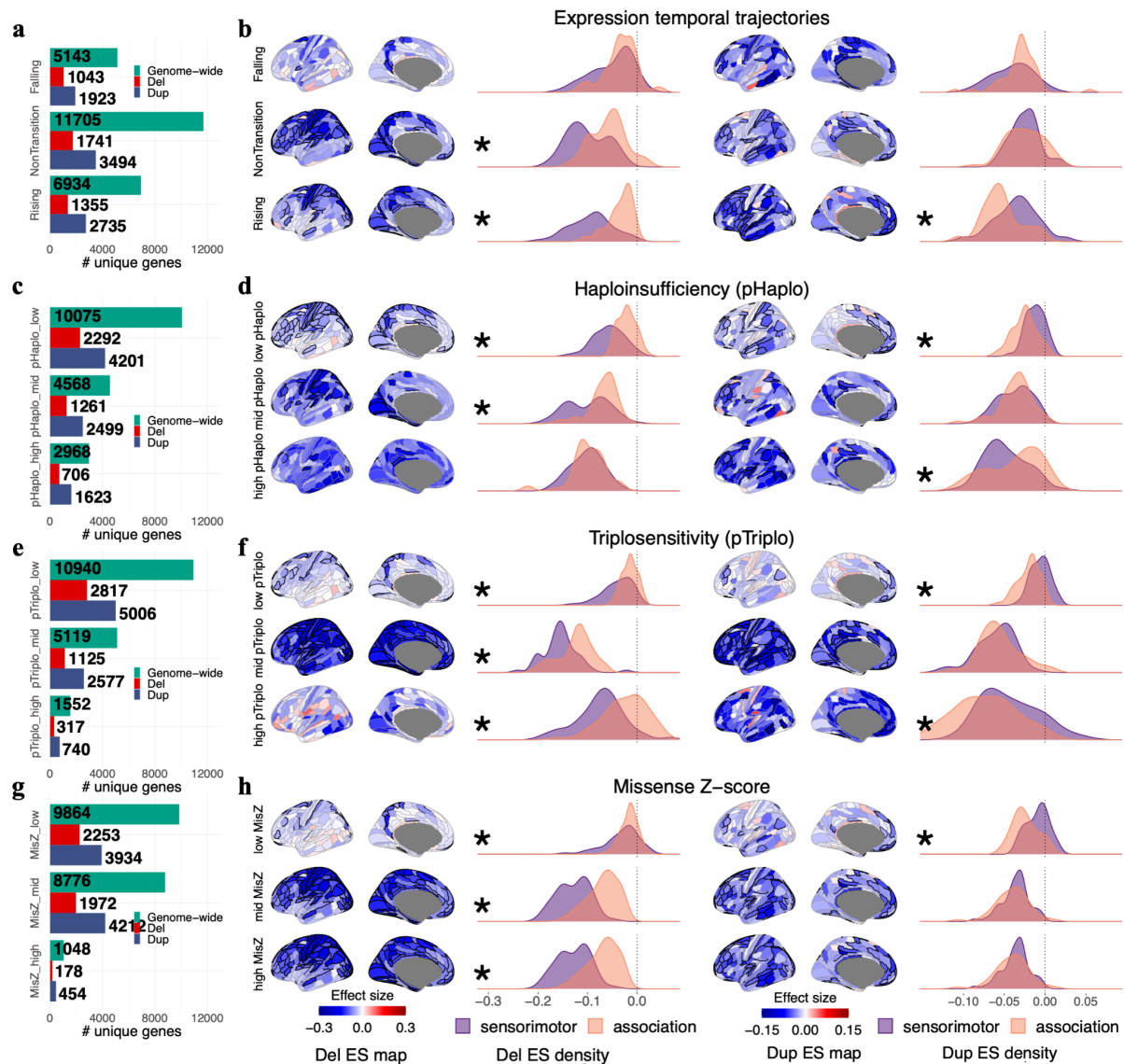


Fig. S9. Characterizing the impact of temporal gene expression trajectories, haploinsufficiency score, triplosensitivity score, and Missense-Zscore.

Legend: Barplot showing the number of genes for **a**) temporal expression trajectory categorized into falling, non-transitional, and rising; **c**) three categories defined by stratifying the probability of haploinsufficiency (pHaplo) score; **e**) three categories defined by stratifying the probability of triplosensitivity (pTriplo) score; and **g**) three categories defined by stratifying the Missense Z-score. Number (#) of unique genes observed in deletions (red) and duplications (blue) in our assembled data, as well as genome-wide (green, as reported

in the resource paper).

Effect sizes maps of cognitive ability and density plots comparing effect sizes of sensorimotor and association regions for deletions (left) and duplications (right) for **b)** three non-overlapping categories of expression temporal trajectory; **d)** three non-overlapping categories of pHaplo; **f)** three non-overlapping categories of pTriplo; and **h)** three non-overlapping categories of Missense Z-score. *: represents a significant difference between the sensorimotor and association cortical region effect sizes; Kolmogorov–Smirnov test $p\text{-value} < 0.05$ (FDR corrected). Del: deletion; Dup: duplication; ES: effect size; #: number.

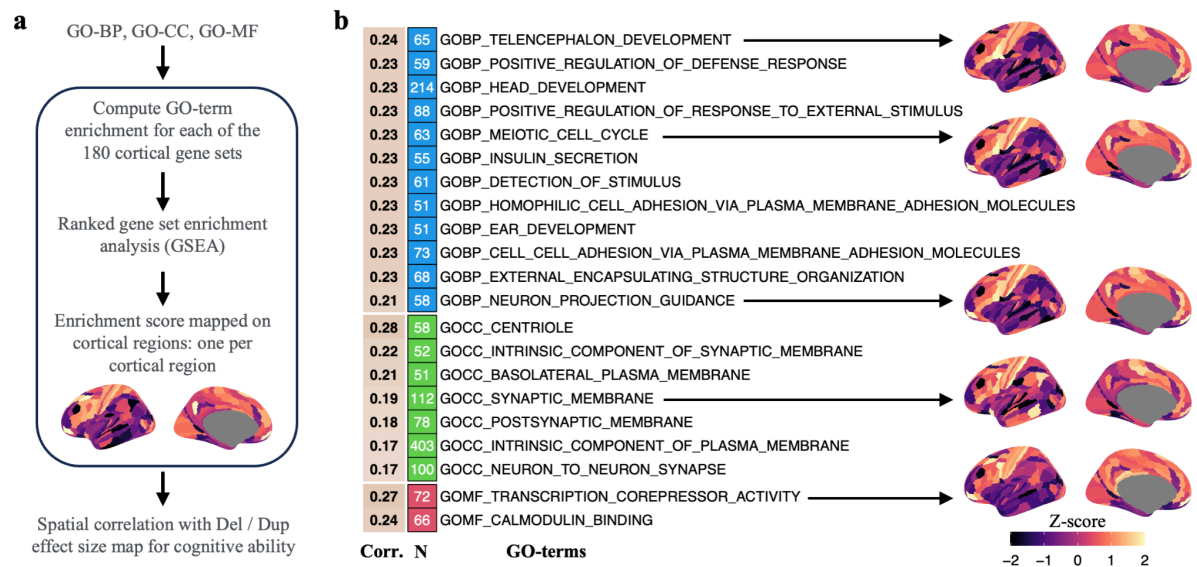


Fig. S10. Enrichment in gene ontologies across cortical gene sets.

a) Methods for i) computing gene ontology (GO) enrichments for each ($n=180$) brain region and corresponding gene-set using ranked gene set enrichment (fgsea package in R); ii) projecting enrichment scores on a cortical map, creating a spatial profile for each GO-term, and iii) spatial correlation with deletion and duplication effect size maps of cognitive ability. Enrichment analyses were performed for 1399 GO terms covering 3 categories: GO-BP: Gene Ontology biological process (1057 terms); GO-CC: Gene Ontology cellular component (177 terms); and GO-MF: Gene Ontology molecular function (165 terms). **b)** Similarity between ontology enrichment maps and the deletion effect size map of cognitive ability. 21 ontology maps showed a significant (spin permutation, FDR $q < 0.05$) correlation with the deletion effect size map. None were correlated with the duplication map. Select brain-maps on the right show the normalized enrichment score (NES) for 180 cortical regions (Z-scored). The number of genes per GO-term query is shown before each GO-term, and color-coded for 3 categories of GO-terms: BP, CC, and MF.

BP: biological process; CC: cellular component; Corr.: Pearson correlation; Del: deletions; Dup: duplications; GO: gene ontology; MF: molecular function.

References

1. Sjöstedt, E. *et al.* An atlas of the protein-coding genes in the human, pig, and mouse brain. *Science* **367**, (2020).
2. Miller, J. A. *et al.* Transcriptional landscape of the prenatal human brain. *Nature* **508**, 199–206 (2014).
3. French, L. & Paus, T. A FreeSurfer view of the cortical transcriptome generated from the Allen Human Brain Atlas. *Front. Neurosci.* **9**, 323 (2015).
4. Markello, R. D. *et al.* Standardizing workflows in imaging transcriptomics with the abagen toolbox. *Elife* **10**, (2021).
5. Wagstyl, K. *et al.* Transcriptional cartography integrates multiscale biology of the human cortex. *eLife* (2023) doi:10.7554/elife.86933.
6. Seguin, C., Razi, A. & Zalesky, A. Inferring neural signalling directionality from undirected structural connectomes. *Nat. Commun.* **10**, 4289 (2019).
7. Sydnor, V. J. *et al.* Neurodevelopment of the association cortices: Patterns, mechanisms, and implications for psychopathology. *Neuron* Preprint at <https://doi.org/10.1016/j.neuron.2021.06.016> (2021).
8. Burt, J. B. *et al.* Hierarchy of transcriptomic specialization across human cortex captured by structural neuroimaging topography. *Nat. Neurosci.* **21**, 1251–1259 (2018).